Proc. of the European Safety and Reliability Conference (ESREL 2026)
Edited by José C. Matos, Paulo B. Lourenço, Michael Beer, Daniel Oliveira, Edoardo Patelli, Hélder S. Sousa, Rui A. Silva and Monica Santamaria

doi: 10.3850/ESREL2026061419_esrel26-p26081-cd

Eliciting the influence of molehills on the stability of river dikes with structured expert judgment

Patricia Mares-Nasarre
Department of Hydraulic Engineering, Delft University of Technology, the Netherlands.
E-mail: p.maresnasarre@tudelft.nl

Robert Lanzafame
GEI Consultants, 180 Grand Ave Suite 950, Oakland, California USA, 94612
E-mail: *rlanzafame@geiconsultants.com*

Zheng Guan
Department of Geoscience and Engineering, Delft University of Technology, the Netherlands.
E-mail: z.guan@tudelft.nl

Oswaldo Morales-Nápoles
Department of Hydraulic Engineering, Delft University of Technology, the Netherlands.
E-mail: o.moralesnapoles@tudelft.nl

Earth embankments (e.g., dams, dikes and levees) are critical components of flood defense systems, providing protection against riverine and coastal inundation. The integrity of these structures can be compromised by biotic factors such as burrowing activity from rodents, foxes, and other animals, whereby excavation of the burrows can negatively impact the structure by altering seepage paths and creating defects in the surface that lead to higher turbulence during overflow events and exacerbating pore pressure. Therefore, burrowing activity can contribute to failure of these structures through mechanisms such as slope instability or localized erosion. Despite being a recognized risk, incorporating the influence of animal burrows in the design phase is difficult because of two main reasons: (1) no standardized methodologies exist, to the authors' knowledge, to translate burrow activity into engineering parameters (variables), and (2) numerical methods that could be used to perform a conventional geotechnical design require quantifiable parameters such as hydraulic conductivity, or geometry of discontinuities, which are typically unknown or impractical to measure in the field. In cases where animal burrows are present, these parameters are not easy to measure or predict due to their high variability and limited literature on the topic. In this study, Structured Expert Judgement using Cooke's method is explored as a tool to quantify geotechnical parameters to incorporate burrowing activity in embankment design, focusing on the case of mole activity. The questionnaire includes calibration questions covering both the activity of moles during the mating season (quantified as density measured on the ground surface), and geotechnical parameters of soil. The questions of interest cover parameters necessary for assessing the influence of molehills on instability and overtopping erosion of embankments. The experts are asked to quantify those parameters without the presence of molehills and with a given density of molehills to allow comparison.

Keywords: embankments, dikes, burrows, structured expert judgment, erosion, flood defenses.

1. Introduction

Dikes, levees, or embankments are earthen structures built to protect an area of land from riverine and coastal flooding, being critical components of flood defense systems. The structural integrity of earth embankments can be compromised by biotic factors such as the burrowing activity from rodents, foxes, and other animals (Bayoumi and Meguid, 2011). This burrowing activity can contribute to failure of these structures through mechanisms such as internal erosion, slope instability or localized erosion (Orlandini et al., 2015; Palladino et al., 2020). Excavation of burrows can alter seepage paths and create superficial defects that can lead to increased pore pressures and higher turbulence during overflow events. Consequently, several failures of levees or embankments worldwide have been partially or fully related to the presence of animal activity (e.g.: Bayoumi and Meguid, 2011; Tarrant et al., 2018).

Despite the existence of methodologies for the probabilistic design for earth embankments (e.g.: Vrijling, 2001), which are capable of incorporating a wide variety of factors and analytic approaches, to the authors' knowledge, there is no standardized methodology to incorporate the influence of animal burrows in the design of these structures. This is possibly due to the fact that the numerical methods that could be used to perform a conventional geotechnical design require quantifiable parameters such as hydraulic conductivity, or geometry of discontinuities (Cobos Roa et al., 2014). These parameters are typically unknown or impractical to measure in the field and, if animal burrows are present, they become even more complicated to measure or predict due to their high variability and limited literature on the topic.

Structured expert judgment is an alternative to quantify the uncertainty of variables of interest based on experts' opinions when data is scarce or unfeasible to collect. Cooke's method, also called the Classical method (Cooke, 1991), is a structured expert judgment method that assigns a weight to each expert based on their performance when estimating the uncertainty in a number of seed questions. These weights are then used to aggregate the experts' uncertainty estimates for the variables of interest, thus, assuming that the performance for the seed questions is representative for the questions of interest. The Classical method has been previously applied to support hydraulic structure design in applications such as the assessment of reservoir performance (Fathy et al., 2024), the reconstruction of historical records of water levels in a river (Kindermann et al., 2020) or the estimation of the probabilities of failure of dikes (earthen embankements) for the Dutch part of the Rhine River (Rongen et al., 2022).

In this study, Structured Expert Judgement using Cooke's method is explored as a tool to quantify geotechnical parameters to incorporate burrowing activity in embankment design, focusing on the case of molehills.

2. Methodology

2.1. *Cooke's method*

Cooke's method (Cooke, 1991) is applied here to elicit and combine experts' opinions. For an extensive description of the method, the reader is referred to Cooke and Goossens (2008). In Cooke's method, each expert provides uncertainty estimates for each question through specification of specific percentiles, typically 5%, 50% and 95%. The expert provides those estimates for two types of questions: (1) calibration or seed questions, and (2) questions of interest. Calibration questions are those for which data exists and are, thus, used by the analysts to calibrate the experts. The questions of interest are those that actually want to be elicited.

Here the implementation of the Classical model in the python package ANDURYL ('t Hart et al., 2019; Rongen et al., 2020) is used.

2.1.1. *Calibration*

Given that 3 quantiles are elicited, realizations of the calibration questions should fall on one of the 4 inter-quantile intervals with probability vector $p = (0.05, 0.45, 0.45, 0.05)$. This probability vector can be compared with the sample distribution of the expert's inter-quantile intervals $s(e)$ computed as

$$
\begin{aligned}
s_1(e) &= \#\{i | x_i \leq 5\% \; quantile\}/N \\
s_2(e) &= \#\{i | 5\% < x_i \leq 50\% \; quantile\}/N \\
s_3(e) &= \#\{i | 50\% < x_i \leq 95\% \; quantile\}/N \\
s_4(e) &= \#\{i | 95\% < x_i \; quantile\}/N \\
s(e) &= (s_1, s_2, s_3, s_4)
\end{aligned}
\tag{1}
$$

where x_i denotes calibration question number i and N is the total number of calibration questions. Note that $s(e)$ is computed per expert. The calibration score of each expert $Cal(e)$ can be then computed to assess the discrepancy between p and $s(e)$ as

$$Cal(e) = 1 - \chi^2_3(2NI(s,p)) \tag{2}$$

$$I(s,p) = \sum_{i=1}^{4} s_i \ln(s_i/p_i)$$

where N is the number of calibration questions. Low scores of $Cal(e)$ mean that the expert's assessment is unlikely to be statistically accurate.

2.1.2. *Information*

The information score $Inf(e)$ measures the degree to which the distribution of an expert is concentrated and is defined as

$$Inf(e) = \frac{\sum_{j=1}^{m} I_j(e)}{m} \tag{3}$$

where m is the total number of questions and $I_j(e)$ is given by

$$\begin{aligned} I_j(e) = 0.05 \ln \frac{0.05}{q_5 - L^*} + 0.45 \ln \frac{0.45}{q_{50} - q_5} \\ + 0.45 \ln \frac{0.45}{q_{95} - q_{50}} + 0.05 \ln \frac{0.05}{U^* - q_{95}} \\ + \ln(U^* - L^*) \end{aligned} \tag{4}$$

where q_5, q_{50} and q_{95} are the elicited 5th, 50th and 95th quantiles for question j by expert e, $L^* = L - k(U - L)$ and and $U^* = U + k(U - L)$, with L and U being the lowest and highest value, respectively, obtained from the different experts and the realization if available and $k = 0.1$.

A high score of $Inf(e)$ means that the expert distribution is concentrated in a small region. $Inf(e)$ can be calculated using all the elicited questions, $Inf(e)_{all}$, or based only on the calibration questions, $Inf(e)_{cal}$.

2.1.3. *Aggregation of experts*

Once $Cal(e)$ and $I_j(e)$ are calculated, they are combined into the Combined Score as

$$CS(e) = Cal(e) \cdot Inf(e) \tag{5}$$

$CS(e)$ is used to combine experts opinions, resulting in an aggregated assessment called a "decision maker" (DM). Various decision makers can be formulated, the goal of which is to produce an aggregated assessment that is better than simple averaging and not worse than the best expert; see Cooke and Goossens (2008) for a complete discussion. If the same weight is given to all experts, regardless of performance, it is called Equal Weight Decision Maker (DM_{EW}). Another option is to calculate the weights of the experts based on their $CS(e)$ as

$$w_i = \frac{CS(e_i)}{\sum_{j=1}^{N} CS(e_j)} \tag{6}$$

where w_i represents the weights for the expert i. This is called Decision Maker with Global Weights without optimization (DM_{GN}). It is also possible to restrict the aggregation to experts with $Cal(e) > 0.05$ are considered in the calculations, called Decision maker with Global Weights with optimization (DM_{GO}). Using the computed weights, the probability density function, PDF, and the cumulative distribution function, CDF, for a Decision Maker (f_{DM} and F_{DM}, respectively) are given by

$$f_{DM} = \sum_{i=1}^{N} w_i f_i \tag{7}$$

$$F_{DM} = \sum_{i=1}^{N} w_i F_i$$

where f_i, F_i and w_i refer to the PDF, CDF and the weight of the expert i, respectively.

2.2. *Questionnaire description*

The questionnaire for this study is composed of 12 calibration questions and 8 questions of interest. Calibration questions are organized by the location of each case study, an overview of which is provided in Figure 1; all case studies are located in the Netherlands.

The first 6 questions are calibration questions of the case studies of *Tholen*, *Waarde* and *Ritthem* and are focused on the mole activity, including aspects such as density of molehills, distances between neighboring molehills, or changes dur-

Fig. 1. Case study locations of the calibration questions.

ing the matting season. Question 7 is a calibration question located in *Hoedekenskerke* and asks about the thickness of the layer of clay protecting an embankment. Questions 8 to 12 are also calibration questions and are focused on geotechnical properties of clay at locations *Groeneveldse polder*, *Duifpolder* and *Noord Kethelpolder*. They include soil properties such as the natural water content, the plasticity index or the undrained shear strength.

Questions 13 to 17 are questions of interest that assess the erosion in the inner slope of a grass-covered embankment due to overtopping with and without the presence of molehills. Overtopping is caused by a wave storm that lasts for 6 hours with a spectral significant wave height $H_{m0} = 2$ m, a spectral period $T_{m-1,0} = 7$ s. The cross section of the embankment is shown in Figure 2. Finally, questions 18 to 20 quantify phreatic levels in the inner slope of the embankment with and without the presence of burrows in the inner and outer slope.

Information needed for the calibration questions was retrieved from field campaigns where the retrieved samples were tested in the laboratory (Heijens, 2025; Stichting Toegepast Onderzoek Waterbeheer (STOWA), 2023).

The experts who participated in the elicitation are presented in Appendix A in Table 4.

3. Results

3.1. *Experts' performance and decision makers*

Scores of the Classical model for the experts are shown in Figure 1. Overall, $1.15 \times 10^{-7} \leq Cal(e) \leq 0.47$ with two experts with $Cal(e) > 0.05$ and two more experts with $Cal(e) > 0.01$.

Table 1. Scores of the Classical model for the experts (7 first rows) and decision makers (last three rows).

Expert ID	Cal(e)	$Inf(e)$ All	$Inf(e)$ Seed	Combined
A	0.036	1.93	2.21	0.080
B	1.15×10^{-7}	2.59	3.29	3.78×10^{-7}
C	0.30	1.46	1.45	0.43
D	5.60×10^{-7}	2.34	3.12	1.74×10^{-6}
E	0.0016	1.65	2.04	0.0033
F	0.47	1.11	0.89	0.42
G	1.42×10^{-6}	1.83	2.41	3.42×10^{-6}
DM_{EW}	0.13	0.48	0.57	0.073
DM_{GN}	0.47	0.77	0.66	0.31
DM_{GO}	0.47	0.86	0.65	0.31

Figure 3 shows the position of the realization within the expert's quantiles. A high statistical accuracy according to the Classical method implies that the seed variables are distributed according to the p-vector, as defined in Section 2.1.1. For 12 calibration questions, ideally, one realization would be below the 5th percentile, five realizations in between the 5th and the 50th percentiles, five realizations between the 50th and the 95th percentiles, and one above the 95th percentile. Experts C and F present s-vectors (see Eq. (1)) close to that distribution with most of the mass within the 5th and 95th percentiles, thus their higher statistical accuracy. Most experts tend to overestimate the seed variables, leading to a higher concentration of points over the 95th percentile than below the 5th percentile.

Regarding the amount of information provided by the experts, $1.11 \leq Inf(e)_{all} \leq 2.59$. Note that experts C and F are the most accurate ones, but also the least informative experts. Expert B and D are the most informative ones but also

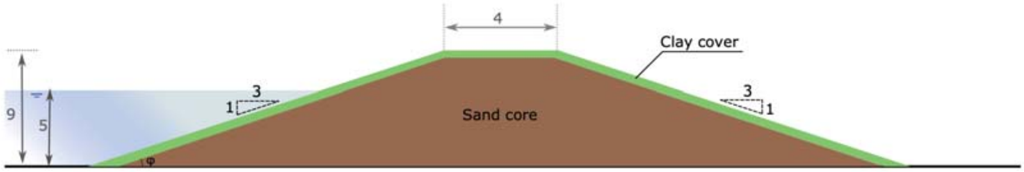

Fig. 2. Cross section of a grass-covered dike. Dimensions in meters.

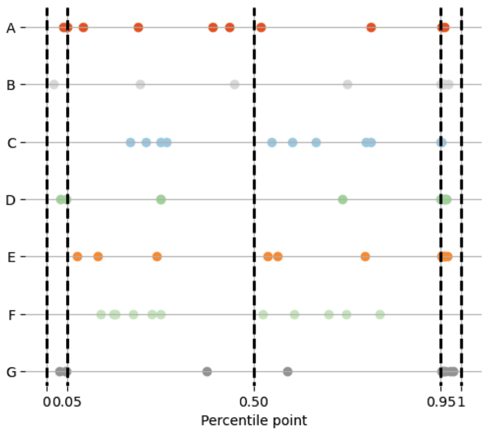

Fig. 3. Realization of the seed questions as percentile of the expert's distribution estimates.

within the least accurate experts.

The scores of the Classical model for the three decision makers are shown in Table 1. The difference between DM_{GN} and DM_{GO} is marginal, which means that excluding experts with $Cal(e) < 0.05$ does not influence the final performance of the decision maker. The decision maker computed with equal weights for all the experts, DM_{EW}, is significantly less accurate and slightly less informative than DM_{GN} and DM_{GO}. Due to the close results between DM_{GN} and DM_{GO}, only the results for DM_{GO} are shown in the following sections.

3.2. *Robustness analysis*

The robustness of the results is calculated by excluding up to 4 items for DM_{GO}. The variation in Calibration Score for removing up to four items is shown in Figure 4.

Figure 4 shows that the results are quite stable for excluding items. The expected value of

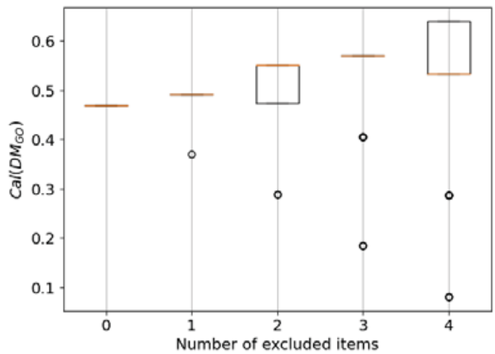

Fig. 4. Robustness analysis for the Calibration Score of DM_{GO}.

$Cal(DM_{GO})$ slightly increases as a higher number of items is removed. As expected, its variability increases with an increasing number of excluded items, though it remains $Cal(DM_{GO}) > 0.05$ regardless of the excluded items.

The variation in Information Score for removing up to four items is shown in Figure 5.

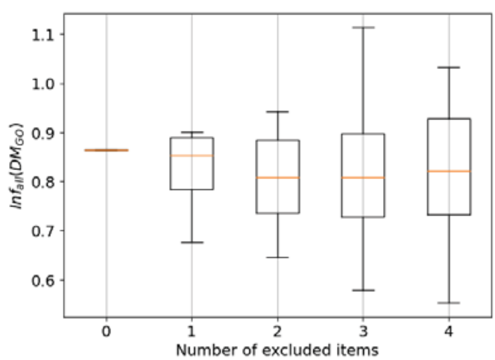

Fig. 5. Robustness analysis for the Information Score of DM_{GO}.

Similarly to the Calibration Score, Figure 5 shows that the Information Score for DM_{GO} is quite stable. The expected value of $Inf_{all}(DM_{GO})$ slightly decreases with an increasing number of excluded items. As expected, its variability increases with an increasing number of excluded items, though it remains $Inf_{all}(DM_{GO}) > 0.5$ regardless of the excluded item.

3.3. *Overtopping erosion*

Figure 6 presents the distributions of erosion depth in the land slope (e_d) without molehills ($e_{d,no}$) and with a molehill ($e_{d,M}$) estimated by the experts and the decision makers, DM_{GO} and DM_{EW}. Table 2 presents the values of e_d whose non-exceedance probability is 0.50 and 0.90 estimated using the distributions elicited from the experts and decision-makers DM_{EQW} and DM_{GO}.

Table 2. Erosion depth in the land slope without molehills ($e_{d,no}$) and with a molehill ($e_{d,M}$) in meters corresponding to a non-exceedance probability of 0.50 and 0.90 estimated by the experts and decision makers.

	50th percentile		90th percentile	
Expert ID	$e_{d,no}$	$e_{d,M}$	$e_{d,no}$	$e_{d,M}$
A	0.15	0.60	0.33	0.96
B	0.0001	0.60	0.09	0.96
C	0.10	0.30	0.28	2.70
D	0.15	0.70	0.28	1.06
E	0.20	0.25	0.47	0.52
F	0.10	0.30	0.90	2.70
G	0.05	0.10	0.09	0.28
DM_{EW}	0.077	0.45	0.35	1.11
DM_{GO}	0.10	0.30	0.58	2.52

As shown in Figure 6, experts agree that the presence of a molehill on the landward slope has influence to some extent in e_d; the molehill makes the erosion more severe. According to the experts, the 50th percentiles fall within $0.001 < e_{d,no}(m) < 0.20$ and $0.10 < e_{d,M}(m) < 0.70$, implying differences between $0.25 < (e_{d,M} - e_{d,no})/e_{d,no} < 6$. Therefore, although all experts agree on the exacerbation of erosion due to the presence of molehills, there is no clear agreement on the magnitude of such effect on $e_{d,M}$.

Regarding the decision-makers, higher differences between DM_{EW} and DM_{GO} are observed for $e_{d,M}$, as shown in Figure 6. For both $e_{d,no}$ and $e_{d,M}$, the differences between DM_{EW} and DM_{GO} become stronger with increasing percentiles.

3.4. *Phreatic levels in the embankment*

Table 3 presents the 90th percentile of PL estimated using the distributions elicited from the experts and decision-makers DM_{EQW} and DM_{GO}.

Table 3. Phreatic levels in the land slope without molehills, PL_{no}, and with a molehill in the water side, PL_w, and land side, PL_L, in meters corresponding to a non-exceedance probability of 0.90 estimated by the experts and decision makers.

Expert ID	PL_{no}	PL_w	PL_L
A	1.44	2.44	3.83
B	1.69	2.44	0.94
C	0.64	0.92	0.91
D	0.89	4.39	2.39
E	1.89	2.39	1.89
F	0.45	0.48	0.28
G	6.89	7.44	7.94
DM_{EW}	5.57	6.52	6.87
DM_{GO}	0.59	0.84	0.82

All experts indicate that the 90th percentile of PL increases when molehills are present in the water slope, while all experts except B and F indicate an increase of the 90th percentile of PL when molehills are present in the land slope. Also, all experts except A and G believe that the presence of molehills in the water side leads to higher PLs. Overall, there seems to be an agreement on how the presence of molehills influence the phreatic levels, although not in the magnitude of such influence.

Experts F and C quantify the lowest 90th percentiles of PL, while G quantifies the highest 90th percentiles of PL. Large discrepancies appear between DM_{GO} and DM_{EW} due to the high PLs elicited by expert G that are not included in DM_{GO} due to the low calibration score of expert G (see Table 1). According to DM_{GO}, $PL_w \approx PL_L$ and $PL_w > PL_{no}$.

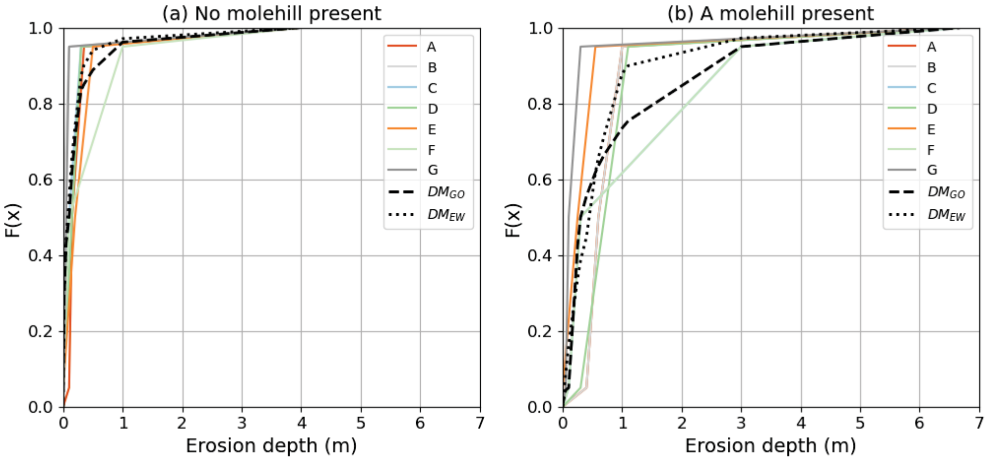

Fig. 6. Distributions of erosion depth in the land side estimated by experts and decision makers: (a) without molehills, and (b) with molehills.

4. Discussion and conclusions

This research proposes a questionnaire to quantify the influence of mole activity on embankment erosion and phreatic levels using structured expert judgment. Seven experts participated in the elicitation.

The experts agree on the influence of molehills in overtopping-driven erosion: it exacerbates erosion. This is in agreement with previous literature on the influence of defects and transitions on dike slopes (e.g.: van Bergeijk et al., 2021; Aguilar-López et al., 2018), where the turbulence generated by the defect or transition makes erosion more severe. However, there is no consensus on the magnitude of such influence between the experts. According to DM_{GO}, the 50th percentile of erosion increases by a factor of 3 if a molehill is present, while the 90th percentile increases by a factor of 4.3. It should be noted that these results are dependent on the conditions of the case study, namely the cross section and storm conditions. Existing methods to estimate overtopping-driven erosion with defects and transitions rely on empirical parameters that need to be empirically calibrated (e.g. Hoffmans, 2012). Further research could compare the results of this study with existing deterministic methods and provide distributions for those empirical parameters.

All experts quantify a difference of the phreatic level in the land slope when molehills are present, except one expert who quantifies no influence in the case of molehills in the land side. However, there is no consensus about where the molehills have a stronger influence on the phreatic levels, water or land side, or the magnitude of such influence. According to Cobos Roa et al. (2014), the presence of burrows close to the foundation in the land side and along the water side leads to a faster saturation of the embankment. Specifically, the burrows in the land side close to the foundation act like a drain which increases the seepage. Based on DM_{GO}, the 90th percentile of the phreatic level increases by factors of 1.42 and 1.39 with molehills present in the water and land side, respectively. Further research could quantify the variations in the phreatic level given not only the number of molehills but also the location where they cluster.

Acknowledgement

The authors acknowledge financial support of the project 'Dieren in de Dijk'. The authors also want to acknowledge the participation of the experts in the study and the support of Danny Janssen and Vana Tsimopoulou in the organization of the elicitation. Finally, authors want to acknowledge Albert Repko, Danny Janssen and Vana Tsimopoulou for facilitating the field data of mole activity.

Appendix A. Experts

Table 4. Experts participating in the elicitation.

Expert name	Description
Anton van der Meer	Researcher in Geotechnical Risk and Reliability at Deltares (Netherlands)
André Koelewijn	Expert on dike technology and monitoring at Deltares (Netherlands)
Wim Kanning	Researcher in Geotechnical Risk and Reliability at Deltares (Netherlands)
Reindert Stellingwerff	Advisor on Flood Defenses at Rijkswaterstaat (Netherlands)
David Knops	Flood Risk consultant at HKV lijn in water (Netherlands)
Gerbert Pleijter	Flood Risk consultant at HKV lijn in water (Netherlands)
Griet de Backer	Geotechnical engineer at Vlaams Ministerie van Mobiliteit en Openbare Werken (Belgium)

References

Aguilar-López, J. P., J. J. Warmink, A. Bomers, R. M. J. Schielen, and S. J. M. H. Hulscher (2018). Failure of grass covered flood defences with roads on top due to wave overtopping: A probabilistic assessment method. *Journal of Marine Science and Engineering 6*(3).

Bayoumi, A. and M. A. Meguid (2011). Wildlife and safety of earthen structures: A review. *Journal of Failure Analysis and Prevention 11*, 295 – 319.

Cobos Roa, D., M. Shriro, N. Sitar, and J. D. Bray (2014). California levee vegetation research program. influence of tree roots and mammal burrowin activity on levee performance: Volume 5. modelling tree roots and mammal burrowing. effects on seepage and stability of levees. Technical report, Geotechnical Engineering, UC Berkley, Report UCB GT 13-03 vol. 5.

Cooke, R. (1991). *Experts in uncertainty: Opinion and subjective probability in science*. Oxford University Press.

Cooke, R. M. and L. L. H. J. Goossens (2008). TU Delft expert judgment data base. *Reliability Engineering System Safety 93*(5), 657–674.

Fathy, M., F. Kazemzadeh Haghighi, and M. Ahmadi (2024). Uncertainty quantification of reservoir performance using machine learning algorithms and structured expert judgment. *Energy 288*, 129906.

Heijens, T. (2025). Mollen graverij in de zeeuwse deijk. Technical report, HZ University of Applied Sciences and Waterschap Scheldestromen.

Hoffmans, G. J. C. M. (2012). *The Influence of Turbulence on Soil Erosion*. Eburon Uitgeverij BV: Delft, The Netherlands.

Kindermann, P. E., W. S. Brouwer, A. van Hamel, M. van Haren, R. P. Verboeket, G. F. Nane, H. Lakhe, R. Prajapati, and J. C. Davids (2020). Return level analysis of the Hanumante River using Structured Expert Judgment: A reconstruction of historical water levels. *Water 12*(11).

Orlandini, S., G. Moretti, and J. D. Albertson (2015). Evidence of an emerging levee failure mechanism causing disastrous floods in Italy. *Water Resources Research 51*(10), 7995–8011.

Palladino, M. R., S. Barbetta, S. Camici, P. Claps, and T. Moramarco (2020). Impact of animal burrows on earthen levee body vulnerability to seepage. *Journal of Flood Risk Management 13*(S1), e12559.

Rongen, G., O. Morales-Nápoles, and M. Kok (2022). Expert judgment-based reliability analysis of the dutch flood defense system. *Reliability Engineering System Safety 224*, 108535.

Rongen, G., C. M. P. 't Hart, G. Leontaris, and O. Morales-Nápoles (2020). Update (1.2) to anduril and anduryl: Performance improvements and a graphical user interface. *SoftwareX 12*, 100497.

Stichting Toegepast Onderzoek Waterbeheer (STOWA) (2023). Landelijke grondparameterset: Afleiden van kentallen voor grondsterkte. Technical report, By Paulina Kindermann and Jan Tigchelaar. STOWA 2023-37. Amersfoort: STOWA.

Tarrant, O., C. Hambidge, C. Hollingsworth, D. Normandale, and S. Burdett (2018). Identifying the signs of weakness, deterioration, and damage to flood defence infrastructure from remotely sensed data and mapped information. *Journal of Flood Risk Management 11*(3), 317–330.

van Bergeijk, V. M., V. A. Verdonk, J. J. Warmink, and S. J. M. H. Hulscher (2021). The cross-dike failure probability by wave overtopping over grass-covered and damaged dikes. *Water 13*(5).

Vrijling, J. K. (2001). Probabilistic design of water defense systems in The Netherlands. *Reliability Engineering System Safety 74*(3), 337–344.

't Hart, C. M. P., G. Leontaris, and O. Morales-Nápoles (2019). Update (1.1) to ANDURIL — a MATLAB toolbox for ANalysis and Decisions with UnceRtaInty: Learning from expert judgments: ANDURYL. *SoftwareX 10*, 100295.